SIMULATION OF THE CYCLIC HARDENING BEHAVIOR OF ALUMINUM ALLOYS

Tayeb KEBIR[1], Mohamed BENGUEDIAB[2], Abdelkader MILOUDI[2], Abdellatif IMAD[3]

The cyclic hardening (stress-strain) curve is useful in the design of structural components that are subjected to cyclic plastic deformation; it is a very important phenomenon that reflects the elastic-plastic material behavior. This work is a contribution to the modeling of low cycle fatigue at a plastic strain imposed for three aluminum alloys (6061-T6, 2024-T3 and 7075-T6) using the ANSYS finite element method. This model has allowed the mechanical characterization in tension and compression of the materials studied and establish their monotonous and cyclic hardening curves. The results are used to determine the constants of Basquin and cyclic hardening parameters. The simulated results are verified against experimental results available in literature.

Keywords: Cyclic hardening, controlled plastic strain, Basquin, low cycle fatigue.

1. Introduction

The strain-hardening generally results in a hardening or sometimes a cyclic softening of a material deformed plastic due to a structural modification. This operation causes an increase in the strength (hardness, yield strength) and a decrease in the ductility (elongation, necking) in the case of sheets, wire and drawn parts.

The aluminum mechanical properties are influenced by its purity and its production method (currying, treating final annealing, etc.).

Several investigations have been devoted to the study of the behavior of metals subjected to large deformations due to hardening. Brammer [1] found that the cyclic hardening is more pronounced for successive imposed deformations. Belattar et al. [2] found that the life of the pre-work-hardened specimens decreases as compared to the one obtained with virgin specimens tests. This reduction is related to the formation of dense dislocation structures inherited from the pre-hardening stage.

[1]PhD Student, Dept. of Mechanical Engineering, University Djillali Liabes of Sidi Bel Abbes, Algeria, e-mail: kebirtayeb@live.fr
[2] Prof., Dept. of Mechanical Engineering, University Djillali Liabes of Sidi Bel Abbes, Algeria, e-mail: benguediabm@gmail.com
[2] Prof., Dept. of Mechanical Engineering, University Djillali Liabes of Sidi Bel Abbes, Algeria, e-mail: miloudidz@yahoo.fr
[3] Prof., Polytech' Lille, University Lille1, France, e-mail:abdellatif.imad@polytech-lille.fr.

The embrittling of microstructure developments during the pre-hardening accelerate fatigue damage and leads to an early break in 304L steel [2]. Recent work led by Désiré et al. [3] on aluminum grades 1200 and 5005 showed that the strong presence of magnesium in 5005 would cause a much more pronounced hardening. The dislocation density in steel (JLF-1) decreases in a cyclic loading deformation imposed with increasing temperature which leads to a low curing [4]. The low cycle fatigue simulations and/or experiments have been performed in the literature mostly for a selected strain amplitude level [5]–[8]. For using nonlinear isotropic/kinematic (combined) hardening a model has been used to predict thermal ratcheting. Kinematic hardening parameters and also isotropic hardening parameters were obtained from the monotonic and cyclic tests at a variety of temperature using controlled strain by Zehsaz et al. [9]. The cyclic hardening or softening behaviors of metallic materials is studied by using many alloys test results [10], [11].

This work is a numerical simulation of the cyclic hardening behavior for determining Basquin's constants and the different parameters of cyclic hardening for three different aluminum alloys 6061-T6, 2024 -T3, and 7075-T6 from the generated hysteresis curves by using the ANSYS finite element method.

2. Controlled cyclic strain

When a specimen is subjected to controlled cyclic strain maximum and minimum constraints are rarely constant throughout the test.

The recording of the force or stress as a function of the deformation provide hysteresis loops (Fig. 1). There are several methods in the literature [12] for determining the cyclic hardening curve.

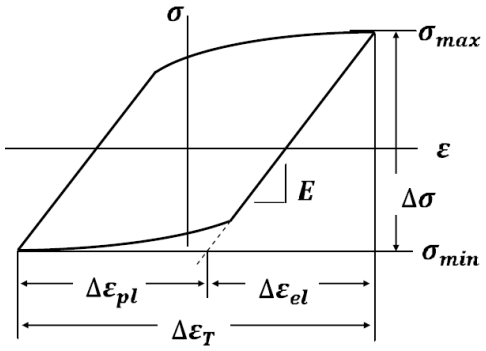

Fig. 1. Hysteresis loops obtained under imposed cyclic strain.

The total strain range ($\Delta\varepsilon_T$) is defined as the sum of the elastic strain range ($\Delta\varepsilon_{el}$) and plastic ($\Delta\varepsilon_{pl}$) strain range.

$$\Delta\varepsilon_T = \Delta\varepsilon_{el} + \Delta\varepsilon_{pl} \tag{1}$$

There are two strain components that make up the cyclic stress-strain curve, which are the linear-elastic portion ($\Delta\varepsilon_{el}$) and the plastic stress-strain ($\Delta\varepsilon_{pl}$).

The linear-elastic strain is given by Eq. (2) for a uniaxial stress state as a function of the elastic modulus (E),

$$\Delta\varepsilon_{el} = \frac{\sigma}{E} \tag{2}$$

The plastic strain (ε_{pl}), is given by Eq. (3) as a function of the strain hardening coefficient (K'), and the strain hardening exponent (n'),

$$\Delta\varepsilon_{pl} = \left(\frac{\sigma}{K'}\right)^{\frac{1}{n'}} \tag{3}$$

The combined elastic and plastic strains constitute the total strain that is known as the cyclic stress-strain equation,

$$\Delta\varepsilon_T = \frac{\sigma}{E} + \left(\frac{\sigma}{K'}\right)^{\frac{1}{n'}} \tag{4}$$

Likewise, the strain-life equation is made up of elastic and plastic terms. The elastic strain-life term is known as Basquin's Equation [13], [14],

$$\frac{\Delta\varepsilon_{el}}{2} = \frac{\sigma'_f}{E}(2N_f)^b \tag{5}$$

Where (σ'_f) is the fatigue strength coefficient, b is the fatigue strength exponent, E is the elastic modulus and (N_f) the number of cycles to failure.

The plastic strain-life term is known as the Coffin-Manson Equation [13], [14].

$$\frac{\Delta\varepsilon_{pl}}{2} = \varepsilon'_f (2N_f)^c \tag{6}$$

Where (ε'_f) is the strain ductility coefficient, c is the strain ductility exponent.

The combined total strain equation is known as the strain-life equation,

$$\frac{\Delta\varepsilon_T}{2} = \frac{\sigma' f}{E}(2N_f)^b + \varepsilon' f\,(2N_f)^c \tag{7}$$

Note that the strain-life equation is defined in terms of cycles.

The cyclic stress-strain curve (Fig. 2) was determined using the method of one specimen for each strain-controlled level and define the stable hysteresis, is obtained by joining the maximum values of each loop [12].

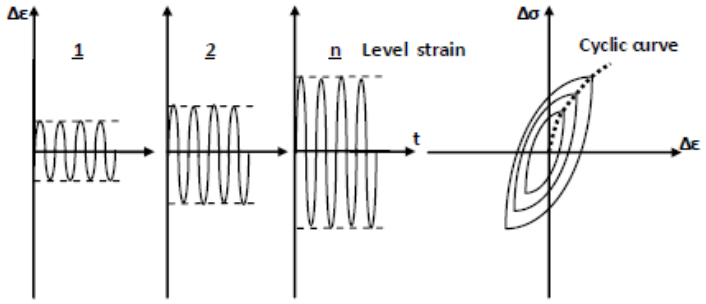

Fig. 2. Determining the cyclic hardening curve [12].

3. Finite Element Modeling

For the low cycle fatigue testing is used a smooth cylindrical specimen subjected to uniaxial forces, done according to the standard test ASTM E606 [15], as presented in Fig. 3.

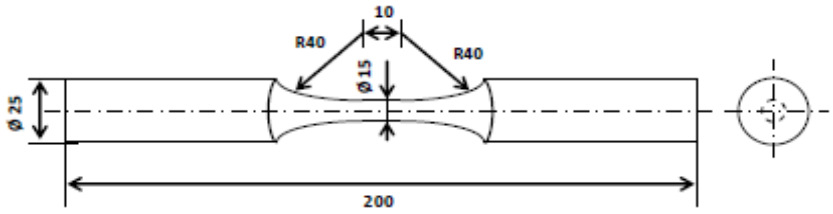

Fig. 3. Geometry and dimensions of the specimens used in the strain-controlled fatigue tests (Dimensions in mm)

The materials studied are aluminum alloys 6061 -T6, 2024 -T3 and 7075-T6 for which chemical compositions are given in Table 1 and mechanical properties are shown in Table 2.

Table 1

Chemical composition of aluminum alloys (weight %)

Material	Cu	Fe	Si	Cr	Mg	Mn	Zn	Ti	References
6061-T6	0.15	0.7	0.4	0.35	0.84	0.14	0.25	0.15	[16]
2024-T3	4.82	0.18	0.07	0.02	1.67	0.58	0.06	0.15	[17], [18]
7075-T6	1.20	0.50	0.40	0.18	2.10	0.30	5.10	0.20	[19]

Table 2

Static mechanical properties

Material	Young's modulus E (GPa)	Poisson's ratio υ	Yield strength σ_y (MPa)	Ultimate tensile strength σ_u (MPa)	Elongation ε_f (%)	References
6061-T6	68	0.30	279	310	14	[20]
2024-T3	72	0.33	370	536	16,7	[18]
7075-T6	70.6	0.30	533	578	14	[21]

The cyclic properties are reported in Table 3.

Table 3

Cyclic mechanical parameters

Material	Fatigue strength coefficient σ'_f (MPa)	Fatigue ductility coefficient ε'_f	Fatigue strength exponent b	Fatigue ductility exponent c	References
6061-T6	705	2.40	-0.11	-0.98	[1]
2024-T3	850	0.22	-0.086	-0.462	[18]
7075-T6	689	0.11	-0.145	-0.509	[21]

The simulation of the cyclic behavior at different controlled strain levels is carried out with a stress ratio R = -1.

The simulation procedure is to set the test specimen on one side and cyclically loaded on the other side by imposed displacement amplitude (ΔL) at a frequency of 2 Hz as shown in Fig. 4. The value of plastic displacement amplitude (ΔL) can be determined by relation Eq. (8).

$$\Delta L = \varepsilon . L \tag{8}$$

Where (ε) is strain and (L) its initial length of test specimen equal 200mm.

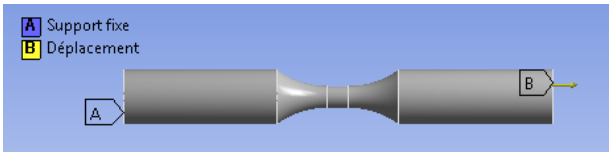

Fig. 4.Displacement applied in test specimen.

For each tested alloy a series of low cycle fatigue simulations at controlled plastic strain amplitude were carried out for different levels according to ASTM E606 standard test [15] as shown in Table 4 and Fig. 4.

Table 4

Cyclic plastic strain controlled in %

Material	Strain controlled in %							
6061-T6	0,30	0.40	0.50	0.60	0.70	1	4	7
2024-T3	0.5	1	2	4	8	12	/	/
7075-T6	0.70	1	3	5	7	9	/	/

The mesh used is of type ***Solid185*** with 8 nodes having three degrees of freedom at each node which makes possible to visualize the deformations in three directions. The convergence has been checked as shown in Fig. 5. The model contains 157329 nodes and 37440 elements.

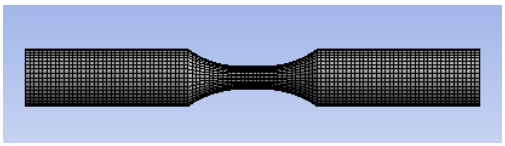

Fig. 5. Test specimen meshing.

The Fig. 6 shows the life time obtained by one simulation to low cycle fatigue for 0.7% controlled cyclic plastic strain in aluminum alloy 7075-T6.

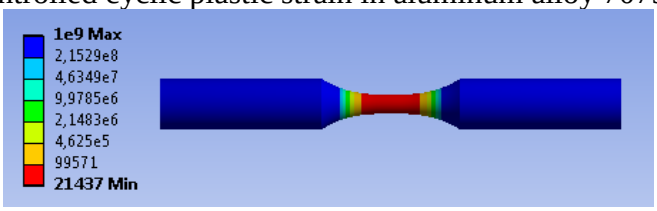

Fig. 6. Lifetime obtained by 0.7% controlled cyclic plastic strain in aluminum alloy 7075-T6.

4. Results and Discussions

Figs. 7, 8 and 9 show the stabilized hysteresis loops for each level of strain imposed for the three tested materials.

The results (Fig. 7a) obtained for the 6061-T6 alloy are explained the simulation hysteresis loops showed good agreement with experimental results, Brammer [1]. Also the Fig. 7b shows the following stable hysteresis loops, measured at different values of strain amplitude for the same material.

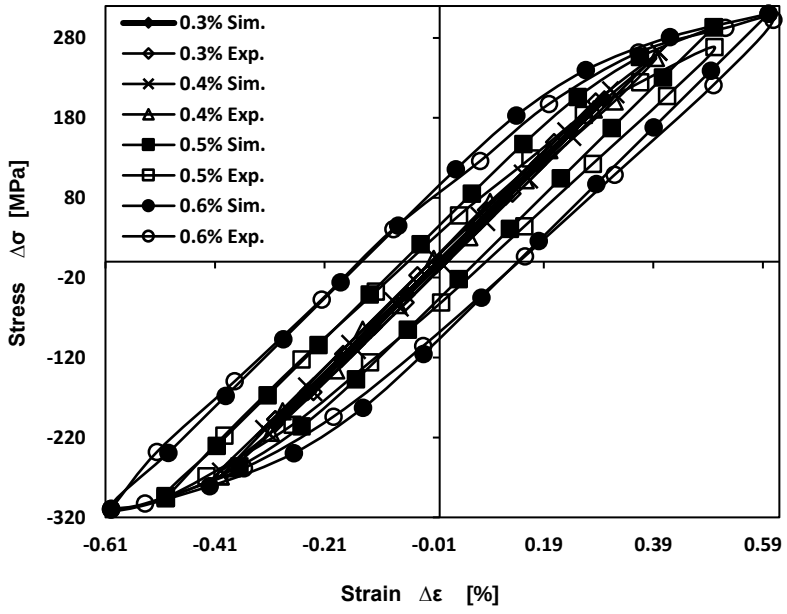

a)

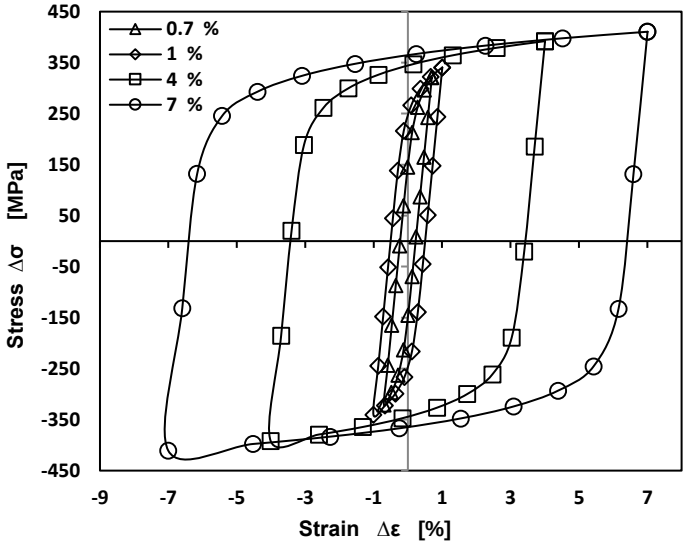

b)

Fig. 7. Simulation of hysteresis loops for 6061 T6 aluminum, a) with experimental results [1], b) without experimental results.

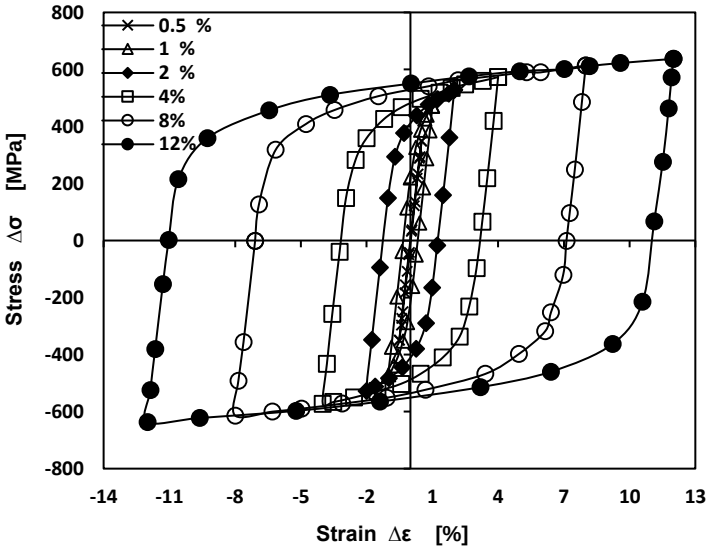

Fig. 8. Simulation of hysteresis loops for 2024-T3 aluminum.

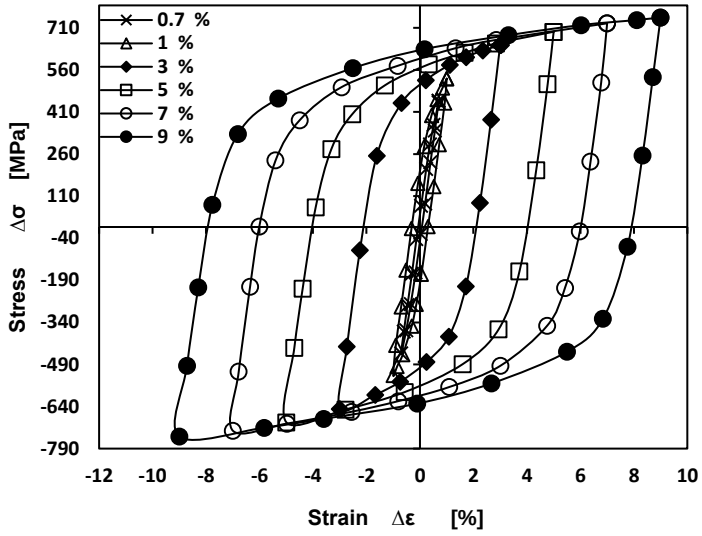

Fig. 9. Simulation of hysteresis loops for 7075-T6 aluminum.

Fig. 10 shows the evolution of the maximum stress on the number (N_f) of cycles to failure for each plastic imposed deformation. These lines obtained can be represented by Basquin's law as:

$$\Delta\sigma/2 = B.(N_f)^A \tag{9}$$

$$Log(\Delta\sigma/2) = A.Log(N_f) + LogB \tag{10}$$

The simulation of hysteresis loops for material 6061 T6 alloy is nearly the same as the ones with experimental results [1].

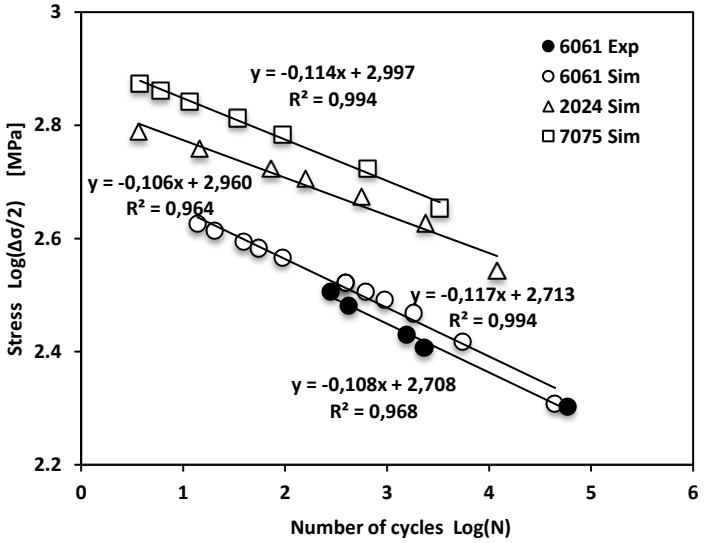

Fig. 10. Plots stress with respect to the number of cycles for the studied alloys.

The coefficients A and B of equation (10) for these alloys are obtained by linear regression as given in Table 5.

Table 5

Constants of Basquin Law.

Material	Simulation		Experimental		
	A	B	A	B	References
6061-T6	-0,117	516,41	-0,108	510,5	[1]
			-0,128	505,9	[20]
2024-T3	-0,106	912,01	-0,112	983	[22]
			-0,182	947,54	[23]
			-0,103	840	[24]
7075-T6	-0,114	993,11	-0,113	985	[22]
			-0,129	1110	[24]

The values of A are between -0.090 and -0.190. These values are comparable to those from the literature for this type of alloy. For each alloy studied, the average values of literature realized a comparison acceptable. The cyclic behavior of these alloys is obtained by plotting the location of the extrema of the hysteresis loops (Figures 7, 8 and 9). The stress-strain diagram is drawn on a curve after passing the initial yield point.

Figures 11 and 12 represent the cyclic hardening curves of the three alloys compared to the curves obtained under monotonic loading.

The simulation of cyclic hardening curve for the 6061 T6 alloy is in good agreement with the experimental results obtained by Brammer [1], (Fig. 11).

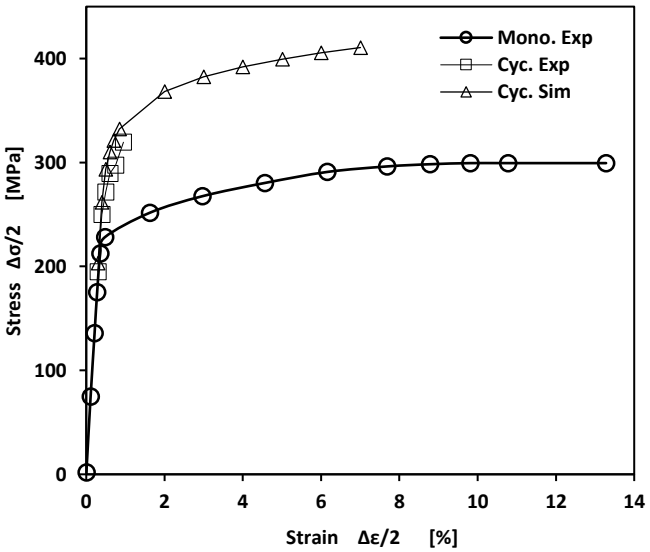

Fig. 11. Cyclic stress-strain curve simulation compared with monotonous and cyclic loading (6061-T6) experimental results [1].

Fig. 12 shows the simulation of cyclic hardening curves for the 2024 T3 and 7075 T6 alloys compared again with experimental monotonous curves [20] and [24], respectively.

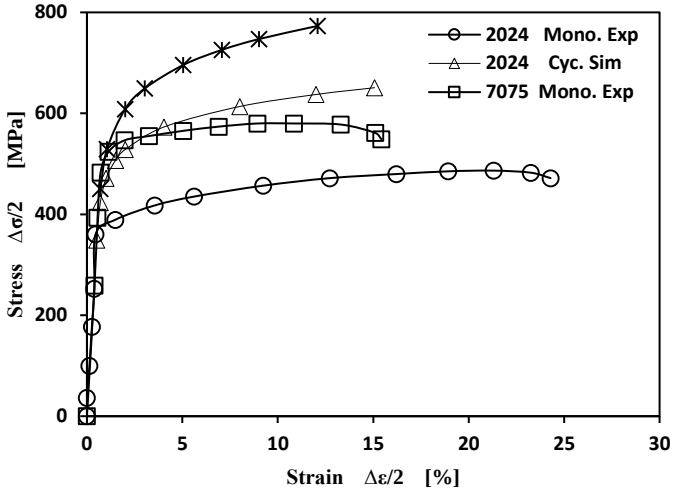

Fig. 12. Cyclic stress-strain curves compared with experimental results monotonic for (Aluminum 2024-T3 [25] and 7075-T6 [21]).

The variations of the cyclic hardening curves can be presented as linear in stress-strain curves which are shown in Fig. 13. The results for 6061 T6 alloy are close to the experimental tests done by Brammer [1].

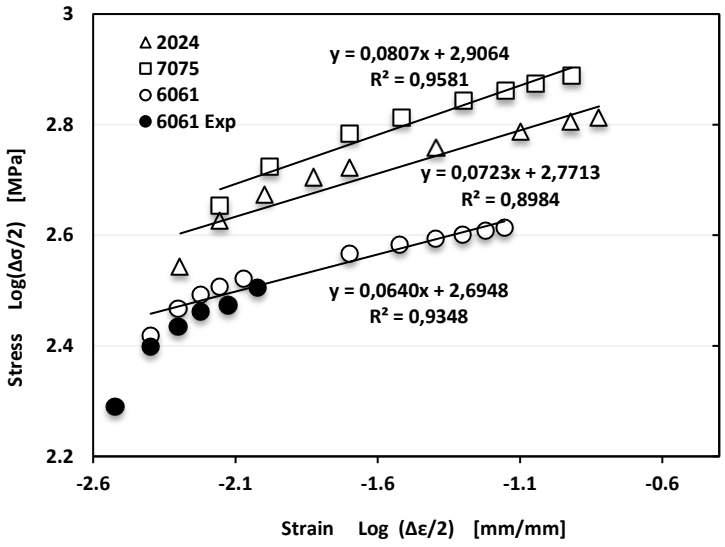

Fig. 13. Evolution of plastic stress-strain.

The representation of the variation of stress in plastic strain can be modeled by power relation (10) as:

$$\Delta\sigma / 2 = K'.(\Delta\varepsilon_{pl} / 2)^{n'} \quad (10)$$

$$Log(\Delta\sigma / 2) = n'.Log(\Delta\varepsilon_{pl} / 2) + LogK' \quad (11)$$

The hardening parameters n' and K' are determined from a linear regression and compared with to those from the literature, are given in Table 6.

The parameter n' is smaller than 0,1 provide a more descriptive way to understand cyclic hardening behavior for this alloys studied.

Table 6

Hardening cyclic parameters

	Simulation		Experimental		
Material	*n'*	*K'*	*n'*	*K'*	References
6061-T6	0.0640	495	0.073	502,8	[1]
2024-T3	0.072	590	0,0651	605,23	[18]
7075-T6	0.0807	806	0,062	790	[21]

6. Conclusions

This work was carried out to model the hardening of three aluminum alloys, 6061-T6, 2024-T3 and 7075-T6 for which the hardening functions were derived from a simulation using ANSYS code. The error observed between the simulations and the experimental results is approximately 3%.

The hysteresis loops are perfectly symmetrical and centered on the point (0,0) in the space of stresses and strains confirming the absence of mean stress and a mean deformation effects during the simulation.

The hysteresis loops for each alloy increase when the imposed plastic strain increases. The increase of the hysteresis areas is explained by the increase of the dissipated plastic deformation energy.

For alloy 6061-T6, the cyclic hardening (stress-strain) behavior obtained from the FE simulation can be clearly compared to experimental tests, [1].

For all studied alloys, the cyclic hardening behavior can be quite different from that obtained under monotonic tensile tests.

The significant hardening observed for 7075-T6 is explained by the high content of magnesium compared to the one in other alloys.

R E F E R E N C E S

[1].*A. T. Brammer*, “Experiments and modeling of the effects of heat exposure on fatigue of 6061 and 7075 aluminum alloys,” Master of science, University of Alabama, 2013.

[2].*A. Belattar, C. Keller, and L. Taleb*, “Etude multi-échelle de l’effet d’un pré- écrouissage en torsion sur le comportement cyclique et la durée de vie en fatigue axiale d’un acier inoxydable 304L à température ambiante,” in *JM’EMP09 EMP, Bordj El Bahri, 08-09 Avril*, 2014, pp. 1–7.

[3].*B. Désiré et al.*, “Modelling of the cyclic hardening of aluminium produced in Cameroon,” *Afrique Sci.*, **vol. 3**, no. 1, pp. 64–78, 2007.

[4].*H. Li, A. Nishimura, T. Muroga, and T. Nagasaka*, “Fatigue life and strain hardening behavior of

JLF-1 steel," *J. Nucl. Mater.*, **vol. 386–388**, pp. 433–436, 2009.
[5].*K. K. G. K. D. Kariyawasam and H. M. Y. C. Mallikarachchi*, "Simulation of Low Cycle Fatigue with Abaqus / FEA," in *3rd International Symposium on Advances in Civil and Environmental Engineering Practices for Sustainable Development*, 2015, pp. 357–364.
[6].*J. D. Ribeiro, A Silva; Moreira da Costa and A. A. Fernandes*, "Low cycle fatigue. Cyclic properties of an Al 6061-T651," in *15th Brazilian Congress of Mechanical Engineering*, 1999.
[7].*A. Ethirajan, M. Saravanan, S. Vishnuvardhan, and J. Jeyanthi*, "Cyclic plastic deformation behaviour of SA 312 type 304LN stainless steel," *Int. J. Eng. Appl. Sci.*, **vol. 2**, no. 5, pp. 2394–3661, 2015.
[8].*D. Lefebvre and F. Ellyin*, "Cyclic response and inelastic strain energy in low cycle fatigue," *International Journal of Fatigue*, **vol. 6**, no. 1, pp. 9–15, 1984.
[9].*M. Zehsaz, F. V. Tahami, and H. Akhani*, "Experimental determination of material parameters using stabilized cycle tests to predict thermal ratchetting," *UPB Sci. Bull. Ser. D Mech. Eng.*, **vol. 78**, no. 2, pp. 17–30, 2016.
[10].*Z. Zhang, J. Li, Q. Sun, Y. Qiao, and C. Li*, "Two parameters describing cyclic hardening/softening behaviors of metallic materials," *J. Mater. Eng. Perform.*, **vol. 18**, pp. 237–244, 2009.
[11].*S. Mroziński and J. Szala*, "Problem of cyclic hardening or softening in metals under programmed loading," *Sci. Probl. Mach. Oper. Maint.*, **vol. 4**, pp. 785–796, 2010.
[12].*M. T. Seyed-Ebrahim*, "Ecrouissage cyclique d'aciers inoxydables austenitique, ferritique et austeno -ferritique : Influence de l'histoire du chargement," PhD Thesis, Université de Lille, 1997.
[13].*R. W. Smith, M. H. Hirschberg, and S. S. Manson*, "Fatigue Behavior of Materials Under Strain Cycling in Low and Intermediate Life Range," *NASA Tech. Note*, pp. 1200–1202, 1977.
[14].*M. Balda*, "Identification of low cycle fatigue parameters," *Appl. Comput.*, **vol. 3**, pp. 259–266, 2009.
[15].*ASTM*, "Standard Test Method for Strain-Controlled Fatigue Testing/Designation: E606/E606M − 12," *ASTM International*, pp. 1–16, 2012.
[16].*I. Philip Maltais*, "Développement d'une méthode de prédiction de la durée de vie en fatigue de structures tubulaires soudées en aluminium," PhD Thesis Université du Québec à Chicoutimi, 2008.
[17].*M. Zehsaz, S. Hassanifard, and F. Esmaeili*, "Fatigue life estimation for different notched specimens based on the volumetric approach," in *EPJ Web of Conferences*, 2010, pp. 1–10.
[18].*Karakaş and J. Szusta*, "Monotonic and low cycle fatigue behaviour of 2024-T3 aluminium alloy between room temperature and 300 °C for designing VAWT components," *Fatigue Fract. Eng. Mater. Struct.*, **vol. 39**, pp. 95–109, 2016.
[19].*M. Aissani*, "Étude du comportement thermique et mécanique des matériaux aéronautiques par des méthodes numériques : application au soudage de structures métalliques," PhD Thesis Université de Blida, Algerie, 2012.
[20].*R. R. Ambriz and D. Jaramillo*, "Mechanical behavior of precipitation hardened aluminum alloys welds," *INTECH*, pp. 36–58, 2014.
[21].*J. Colin*, "Deformation history and load sequence effects on cumulative fatigue damage and life predictions," PhD Thesis University of Toledo, 2010.
[22].*A. Fatemi, A. Plaseied, A. K. Khosrovaneh, and D. Tanner*, "Application of bi-linear log-log S-N model to strain-controlled fatigue data of aluminum alloys and its effect on life predictions," *Int. J. Fatigue*, **vol. 27**, pp. 1040–1050, 2005.
[23].*P. Cavaliere, R. Nobile, F. W. Panella, and A. Squillace*, "Mechanical and microstructural behaviour of 2024-7075 aluminium alloy sheets joined by friction stir welding," *Int. J. Mach. Tools Manuf.*, **vol. 46**, pp. 588–594, 2006.
[24].*A. D. Freed and B. I. Sandor*, "A hyperbolic relationship for stress vs life," *fatigue Eng. Mater. Struct.*, **vol. 6**, pp. 377–381, 1983.
[25].*A. Lipski and S. Mrozinski*, "The effects of temperature on the strength properties of aluminium alloy 2024-T3," *Acta Mech. Autom.*, **vol. 6**, no. 3, pp. 62–66, 2012.